Ab Initio Evaluation of Absorption and Emission Transitions for Molecular Solutes, Including Separate Consideration of Orientational and Inductive Solvent Effects

R. Bonaccorsi

Istituto di Chimica Quantistica ed Energetica Molecolare, Consiglio Nazionale delle Ricerche, Via Risorgimento, 35-56100 Pisa, Italy

R. Cimiraglia and J. Tomasi

Istituto di Chimica Fisica, Università di Pisa, Via Risorgimento, 35-56100 Pisa, Italy

An *ab initio* computation procedure to obtain electronic transition wave numbers in solution is presented and discussed. The continuum description of the bulk solvent is adopted, and solute–solvent interaction is reduced to a closed-form interaction operator added to the solute Hamiltonian. The resulting Schrödinger equations are solved variationally. No limitations are imposed on the shape of the solvent cavity or on the level of accuracy of the *ab initio* procedure.

I. INTRODUCTION

Current theories[1-8] for solvent effect on electronic spectra in dilute solutions are based on a second-order perturbation approximation where it is assumed that solute and solvent molecules are sufficiently well separated in order that the mutual overlap of electronic distributions can be ignored. The basic expression is then further elaborated to get manageable formulas of practical use.[9]

Among the simplifications introduced in this way, of particular interest is the adoption of the Onsager model for solute–solvent interactions.[10] The use of this model has a twofold consequence; it gives, via the introduction of the reaction field created by a continuum representation of the solvent, a reasonable account of the necessary configurational average of the solvent molecules around the solute, and it reduces the solute–solvent interaction to the lowest terms of an expansion, represented by the solute dipole moment and polarizability. These two features are not inherently connected, and it is possible to consider alternative formulations in which, for example, the continuous dielectric model of the solvent is maintained and more accurate descriptions of the solute–solvent interactions are introduced.

Recently, we have presented a computational scheme to treat solvent effects in the framework of the continuous dielectric model (hereafter referred to as article I),[11] which is able to represent the corresponding solute–solvent interaction to all the orders of expansion, avoiding the ancillary condition of spherical shape for the cavity, as required by current models.

In the applications of this method thus far published,[12-16] a simplified description of the solvent has been adopted, characterized by the static dielectric constant ϵ alone, which does not make distinction between orientational and inductive polarization of the solvent. Current methods for the evaluation of solvent effects on electronic spectra give emphasis, on the contrary, to these two contributions in the solvent polarization. A modification of the computational scheme of article I is presented here, which is able to treat these two contributions separately. It must be stressed that with this procedure the evaluation of the electronic transitions is no longer related to a second-order perturbation theory, all the pertinent Schrödinger equations being solved variationally. As in current theories for solvent electronic shifts, the description of the bulk solvent in terms of a continuous dielectric characterized by suitable macroscopic, temperature-dependent,

quantities is here accepted, as well as the hypothesis of sufficiently large separation between molecules in solution. Extension to cases where specific solute–solvent interactions play a non-negligible role can be readily performed by defining as "solute," M, a suitable supermolecular system composed of the true solute and the appropriate number of solvent molecules.

In the present article, attention is focused on the electrostatic interaction terms, and dispersion-repulsion effects will not be considered here.

II. THE BASIC COMPUTATIONAL SCHEME

The basic feature of the computational scheme is given by the introduction in the molecular Hamiltonian $\hat{H}_M^0$ of the solute M of an electrostatic interaction operator $\hat{V}_\sigma$. From the new Hamiltonian $\hat{H}_M = \hat{H}_M^0 + \hat{V}_\sigma$, information on the solvent effect on the properties of ground as well as excited states of M can be extracted. With appropriate manipulations other quantities, such as the changes in the thermodynamical properties due to the solution process, can be evaluated.[15]

The operator $\hat{V}_\sigma$ is the quantum mechanical counterpart of the classical electrostatic potential energy deriving from the potential V_σ, associated with an "apparent" charge density $\sigma(s)$ induced by the solute on the surface of the cavity containing M. V_σ, when calculated with the rigid unperturbed charge distribution $\rho_M^0(\boldsymbol{r})$, is exactly the reaction potential of Onsager, and it may be employed to get a classical evaluation of the free-energy change in the solution process.[12] When V_σ is obtained through an iterative process involving the $\rho_M(\boldsymbol{r})$ charge distribution given by $\hat{H}_M$, it represents the reaction potential produced by the actual solute in the solution.

The charge distribution $\sigma(s)$ is formally related to the normal component of the polarization vector $\boldsymbol{P}$ in the dielectric at the cavity surface:

$$\sigma(s) = -P_{n+} = \frac{\epsilon - 1}{4\pi}\left(\frac{\partial V}{\partial n}\right)_{s_+} \qquad (1)$$

here the vector $\boldsymbol{n}$ is taken on the cavity surface pointing towards the dielectric, and the index $+$ emphasizes the fact that according to this definition the value of $\partial V/\partial n$ refers to the dielectric side in the cavity surface. For practical reasons, it is convenient to exploit a boundary condition on the cavity surface and to write

$$\sigma(s) = \frac{\epsilon - 1}{4\pi\epsilon}\left(\frac{\partial V}{\partial n}\right)_{s_-} \qquad (2)$$

in which the calculation of the gradient of V is performed on the vacuum side of the cavity surface. It must be stressed that V is the total potential acting at position s, i.e. $V = V(\rho) + V(\sigma)$. This fact leads to adopting an iterative procedure, which can be summarized in the following steps:

2.1. Calculation of

$$\sigma^{00}(s) = \frac{\epsilon - 1}{4\pi\epsilon}\left(\frac{\partial V(\rho^0)}{\partial n}\right)_{s_-} \qquad (3)$$

where $V(\rho^0)$ is the electrostatic potential produced by the unperturbed wave function of M.

2.2. Iterative calculation of the surface charge $[\partial V(\sigma)/\partial n]_{s_-}$ contributions to σ, until a final value

$$\sigma^{0f}(s) = \frac{\epsilon - 1}{4\pi\epsilon}\left(\frac{\partial[V(\rho^0) + V(\sigma)]}{\partial n}\right)_{s_-} \qquad (4)$$

is reached.

2.3. Calculation of a solvent-polarized wave function $\psi^{(1)}$ for M, via the Hamiltonian $(\hat{H}_M^0 + \hat{V}_{\sigma^{0f}})$, and consequent changes in $\sigma(s)$. The cycle 2.2–2.3 is repeated until the final value

$$\sigma^{ff}(s) = \frac{\epsilon - 1}{4\pi\epsilon}\left(\frac{\partial[V(\rho^f) + V(\sigma^{ff})]}{\partial n}\right)_{s_-} \qquad (5)$$

is reached.

It may be remarked that this computational scheme allows one to employ the usual variational theorem, though formally we have a term in the Hamiltonian, $\hat{V}_\sigma$, explicitly dependent on the solution $\hat{V}_\sigma = \hat{V}_\sigma(\rho)$. A direct, noniterative, variational solution of the corresponding Schrödinger equation should lead to a reformulation of the energy functional to be extremised in the variational procedure (see Sanhueza et al.[17]).

This computational scheme has been implemented, tested, and described in article I, with the additional approximation of substituting the continuous charge distribution σ (at every level of approximation) by a finite set of point charges q_{Ki} placed at the center of appropriate portions ("tesserae") of the cavity surface, each having a known area ΔS_{Ki}:

$$\sigma(s_{Ki}) = (q_{Ki}/\Delta S_{Ki})\delta^S(\boldsymbol{r} - s_{Ki}) \qquad (6)$$

The double index introduced in eq. (6) refers to a modeling of the cavity surface in terms of an arbitrary number of interlocking spheres, $K, L, \ldots,$ each of which is divided into tesserae with indexes

$i, j, \ldots$, and $\delta^S(\boldsymbol{r} - \boldsymbol{s})$ is a surface δ function of immediate definition.

The computational scheme discussed in article I considered the solvent as an isotropic linear dielectric characterized by its static dielectric constant ϵ alone [see eqs. (2)–(5)]. It is possible, however, to pass to dielectrics characterized by static and frequency dependent dielectric constants $\epsilon(0)$ and $\epsilon(\omega)$.

The polarization vector $\boldsymbol{P}(\boldsymbol{r})$ may be divided into an inductive and an orientational component:

$$\boldsymbol{P}_{\text{tot}} = \boldsymbol{P}_{\text{ind}} + \boldsymbol{P}_{\text{or}} \tag{7}$$

the first corresponding to the polarization of the electronic cloud of the solvent molecules and the second to the difference in orientation of the solvent molecules with respect to a Boltzmann averaged distribution in the bulk solvent. Accordingly, the surface charge distribution may be divided into analogous contributions:

$$\sigma_{\text{tot}} = \sigma_{\text{ind}} + \sigma_{\text{or}} \tag{8}$$

which may be operationally defined as follows:

$$\sigma_{\text{tot}} = [(\epsilon - 1)/4\pi\epsilon](\partial V/\partial n)_{s_-} \tag{9}$$

$$\sigma_{\text{ind}} = [(n^2 - 1)/4\pi n^2](\partial V/\partial n)_{s_-} \tag{10}$$

$$\sigma_{\text{or}} = \sigma_{\text{tot}} - \sigma_{\text{ind}} \tag{11}$$

It may be remarked that there is not a direct definition of σ_{or}. In eq. (10) the notation $n^2 = \epsilon(\infty)$ (n = refractive index at infinite frequency) has been adopted. (In the same expression we have exploited the independence of polarization effects in the dielectric when passing from quantities defined at s_+ to quantities defined at s_-.)

The physical nature of the problem under examination will dictate the details of the computational scheme. The discussion will be limited here to two characteristic cases: vertical absorption from the ground state and emission from an excited state in equilibrium with the solvent. Extension to other cases may proceed through analogous manipulations.

III. VERTICAL EXCITATION PROCESSES

During vertical excitation processes $M(\text{GS}) + h\nu \to M(\text{EX})$, the orientational contribution to $\boldsymbol{P}$ remains constant, while the inductive term experiences the change in the solute charge distribution. Introducing in the notation an explicit reference to the quantities on which σ depends, we have before the absorption:
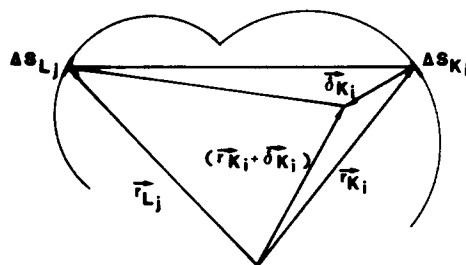
Figure 1. Definitions of the vectors employed in eqs. (15) and (22). The cavity is here represented by a planar section where only two spheres, K and L, are considered. The vectors r_{Ki} and r_{Lj} refer to the positions of surface tesserae centers with respect to an arbitrary internal reference frame. The vectors $\delta_{Ki} \cdots$ are vectors of fixed length lying along the normal to the cavity surface of the centers of the tesserae.

$$\sigma(\text{GS}) = \sigma_{\text{tot}}(\epsilon, \rho_{\text{GS}}) \tag{12}$$

and immediately afterwards:

$$\sigma(\text{EX}) = \sigma_{\text{or}}(\rho_{\text{GS}}) + \sigma_{\text{ind}}(n^2, \rho_{\text{EX}}) \tag{13}$$

A reasonable approximation, which preserves the time-independent formulation, consists in adopting expression (13) for the definition of the solvent interaction operator to be used in the calculation of the electronic excitation energy. An iterative procedure must of consequence be used. The computations may be organized according the following scheme:

3.1 Computation of σ_{tot} and of its components for the GS. The same scheme as in article I may be here employed. Explicit expressions are repeated here for the reader's convenience, and also because there are in the source article some typographical misprints.

3.1.1. The σ distribution is replaced by a finite set of point charges q_{Ki} placed at the center of suitably defined portions of the cavity surface, with area ΔS_{Ki}, according to the following definition [see eqs. (3) and (6)]:

$$q_{Ki}^{00} = [(\epsilon - 1)/4\pi\epsilon](\partial V(\rho^0)/\partial n)_{s_-}\Delta S_{Ki} \tag{14}$$

3.1.2. The iterative introduction of mutual polarization of surface charges is numerically performed by using the expression

$$q_{Ki}^{0,m} = q_{Ki}^{00} - \frac{\epsilon - 1}{4\pi\epsilon}\left\{\frac{\Delta S_{Ki}}{|\delta|}\left[\sum_{Lj \neq Ki} q_{Lj}^{0,m-1}\right.\right.$$

$$\times\left(\frac{1}{|(r_{Ki} - \delta) - r_{Lj}|} - \frac{1}{|r_{Ki} - r_{Lj}|}\right)\right]$$

$$\left.\left. - 2\pi q_{Ki}^{0,m-1}\left(1 + \left(\frac{\Delta S_{Ki}}{4\pi R_K^2}\right)^{1/2}\right)\right\} \tag{15}$$

The vectors r_{Ki}, r_{Lj} and δ are defined in Figure 1.

The last term of the right side of (15) accounts for the self-polarization of the surface charge contained in the tessera ΔS_{Ki}. Reference is made to article I for further details. The experience thus far gained in actual computations suggests limiting the iterative cycle to four steps ($m_{max} = f = 4$).

3.1.3. Compensation of the excess surface charge (ESCC).

The occurrence of "tails" of $\rho_M^0(r)$ going outside the cavity boundaries produces an unbalance between the charge of the solute and that of the cavity surface which leads, if not corrected, to non-negligible errors (see article I). A simple device to eliminate these errors to a good extent consists in multiplying each q_{Ki} element by a compensation factor such that the new set of surface charges has the correct total value ($\Sigma_{q_{Ki}} = 0$ for neutral solutes and $-q_M[(\epsilon - 1)/4\pi\epsilon]$ for solutes with net charge q_M). Several expressions for this factor could be introduced, but we shall maintain the expression given in article I, which distributes an extra charge $-Q$ over all the q_{Ki} charges, according to the magnitude and the sign they have, using for positive q_{Ki}'s the factor

$$g^+ = 1 - \frac{Q}{2Q_+} \qquad (16)$$

and for the negative q_{Ki}'s:

$$g^- = 1 - \frac{Q}{2Q_-} \qquad (17)$$

Q is the excess surface charge (negative) and Q_+ and Q_- are the sum of the positive and negative uncorrected surface charges.

As has been remarked in article I, it would be better to perform the ESCC at the beginning and at the end of the computational cycle. The results are, however, little affected by the number of ESCCs, and the results given in Sec. V refer to ESCC performed only at the end of the cycle.

3.1.4. Calculation of an improved (i.e. polarized) wave function for the GS of M.

From the set of compensated surface charges q_{Ki}^{0f}, it is immediate to derive the operator $\hat{V}(\sigma^{0f})$ which is introduced in the Hamiltonian given in 2.4. All the calculations are here performed at the self-consistent-field (SCF) level, but extension to more sophisticated methods is immediate. With the resulting solute charge distribution, the cycle 3.1.1.–3.1.4 is repeated until stable values are reached. Some examples of convergence are given in article I and in section V of the present article. In routine calculations it may be sufficient to perform two cycles, σ_{tot}^{ff} (GS) $\simeq \sigma_{tot}^{2f}$(GS).

3.1.5. Calculation of the orientational and inductive components of the surface charge, σ_{or}(GS) and σ_{ind}(GS).

Because of the assumed linearity of the two polarization processes, the two sets of surface charges are given by the following relations:

$$q_{Ki,ind}^{ff}(\text{GS}) = r q_{Ki,tot}^{ff}(\text{GS}) \qquad (18)$$

$$q_{Ki,or}^{ff}(\text{GS}) = (1 - r) q_{Ki,tot}^{ff}(\text{GS}) \qquad (19)$$

with

$$r = [(n^2 - 1)/n^2][\epsilon/(\epsilon - 1)] \qquad (20)$$

Both sets of charges are corrected from excess surface charge errors.

3.2. Computation of $\sigma_{ind}(n^2, \text{EX})$.

To do it, it is necessary to pass through an iterative definition of the excited-state charge distribution related to the Hamiltonian

$$\hat{H}_M^0 + \hat{V}[\sigma_{or}^{ff}(\text{GS})] + V[\sigma_{ind}^{ff}(\text{EX})] \qquad (21)$$

The numerical results presented in a following section refer to excited states calculated with the electron-hole potential (EHP) method of Morokuma and Iwata.[18] Other more refined methods to compute excited state wavefunctions could, of course, be employed, but it is probably sufficient to use a rapid and relatively inexpensive method such as the EHP method, to get the final value $\sigma_{ind}^{ff}(\text{EX})$, and then to pass to more complex methods for the final evaluation of the absorption energy. The computational scheme has been arranged as follows.
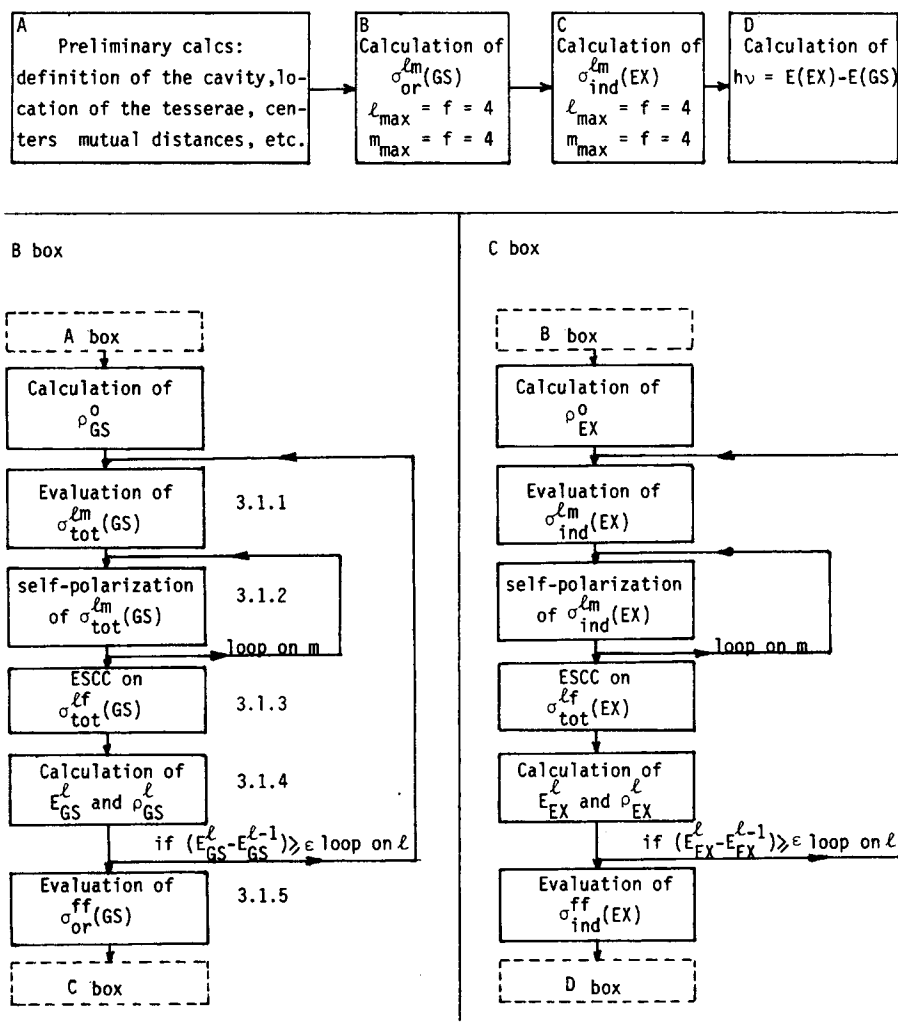
3.2.1. Orientational component of the solvent interaction operator $\sigma_{or}^{ff}(\text{GS})$.

It derives from step 3.1.4.

3.2.2. Inductive component of the interaction operator.

A first set of induction charges, $q_{Ki,ind}^{0f}(\text{EX})$ is obtained by the iterative application of a generalization of eq. (15):

$$q_{Ki,ind}^{0,m}(\text{EX}) = q_{Ki,ind}^{0,0}(\text{EX})$$

$$- \frac{n^2 - 1}{4\pi n^2} \left\{ \frac{\Delta S_{Ki}}{|\delta|} \sum_{Lj}{}' [q_{Lj,or}^{ff}(\text{GS}) + q_{Lj,ind}^{0,m-1}(\text{EX})] \right.$$

$$\times \left(\frac{1}{|(r_{Ki} - \delta) - r_{Lj}|} - \frac{1}{|r_{Ki} - r_{Lj}|} \right)$$

$$- 2\pi[q_{Ki,or}^{ff}(\text{GS}) + q_{Ki,ind}^{0,m-1}(\text{EX})]$$

$$\left. \times \left[1 + \left(\frac{\Delta S_{Ki}}{2\pi R_K^2} \right)^{1/2} \right] \right\} \qquad (22)$$

In this expression the term corresponding to

$$\frac{n^2 - 1}{4\pi n^2} \frac{\partial}{\partial n} [V(\rho_{EX}^0) + V(\sigma_{or}^{ff}(\text{GS}))] \qquad (23)$$

Table I. Flow diagram of the computational scheme for the light absorption processes.

A	B	C	D
Preliminary calcs: definition of the cavity, location of the tesserae, centers mutual distances, etc.	Calculation of $\sigma_{or}^{\ell m}(GS)$, $\ell_{max} = f = 4$, $m_{max} = f = 4$	Calculation of $\sigma_{ind}^{\ell m}(EX)$, $\ell_{max} = f = 4$, $m_{max} = f = 4$	Calculation of $h\nu = E(EX) - E(GS)$

B box

- A box
- Calculation of ρ_{GS}^0
- Evaluation of $\sigma_{tot}^{\ell m}(GS)$ — 3.1.1
- self-polarization of $\sigma_{tot}^{\ell m}(GS)$ — 3.1.2 — loop on m
- ESCC on $\sigma_{tot}^{\ell f}(GS)$ — 3.1.3
- Calculation of E_{GS}^ℓ and ρ_{GS}^ℓ — 3.1.4
- if $(E_{GS}^\ell - E_{GS}^{\ell-1}) \geq \epsilon$ loop on ℓ
- Evaluation of $\sigma_{or}^{ff}(GS)$ — 3.1.5
- C box

C box

- B box
- Calculation of ρ_{EX}^0
- Evaluation of $\sigma_{ind}^{\ell m}(EX)$
- self-polarization of $\sigma_{ind}^{\ell m}(EX)$ — loop on m
- ESCC on $\sigma_{tot}^{\ell f}(EX)$
- Calculation of E_{EX}^ℓ and ρ_{EX}^ℓ
- if $(E_{EX}^\ell - E_{EX}^{\ell-1}) \geq \epsilon$ loop on ℓ
- Evaluation of $\sigma_{ind}^{ff}(EX)$
- D box

is constant, while the iterative calculation regards the contribution to σ deriving from $\sigma_{ind}^0(EX)$. This iterative process converges within few cycles ($m_{max} < 4$). In the first application of expression (22), the excited-state density function (ρ_{EX}^0) comes out from an excited-state calculation related to a Hamiltonian [eq. (21)] in which $\hat{V}(\sigma_{ind}(EX))$ has been replaced by $\hat{V}(\sigma_{ind}^{ff}(GS))$, but one could also use the density function deriving from an *in vacuo* calculation (i.e. with $\hat{H}_M = \hat{H}_M^0$). An ESCC on the final set $q_{Ki,ind}^{0f}(EX)$ is performed (see 3.1.3).

3.2.3. Calculation of an improved value of $\rho(EX)$. The Hamiltonian (21) is employed. The cycle 3.2.2.–3.2.3 is repeated until stable values of $\sigma_{ind}(EX)$ are reached. According to the limited experience thus far gained, a reasonable approximation is reached at the first cycle. For routine calculations it would be sufficient to use $\sigma_{ind}^{1f}(EX)$ or even $\sigma_{ind}^{0f}(EX)$.

3.3. Final calculation. The preceeding step gives the final estimate of the transition energy, and

additional physico–chemical information may be drawn from the corresponding wave function. The final Hamiltonian could be also employed for a more refined definition of the excitation process [e.g. via a large configuration-interaction (CI) procedure]. Our very limited experience indicates that this could be a reasonable strategy. Some attention must be paid, however, when one wants to use V_σ's obtained with a minimal basis in connection with final accurate calculations on a large basis. In many cases the errors introduced in V_σ by the limitations of a poorly balanced minimal basis do not make up for the improvements brought in the final calculations.

For the reader's convenience, a diagrammatic sketch of the procedure is reported in Table I.

IV. EMISSION PROCESSES

We shall now consider the case of emission of light from excited species, supposed to be in

Table II. Flow diagram of the computational scheme for the light emission processes.

B box
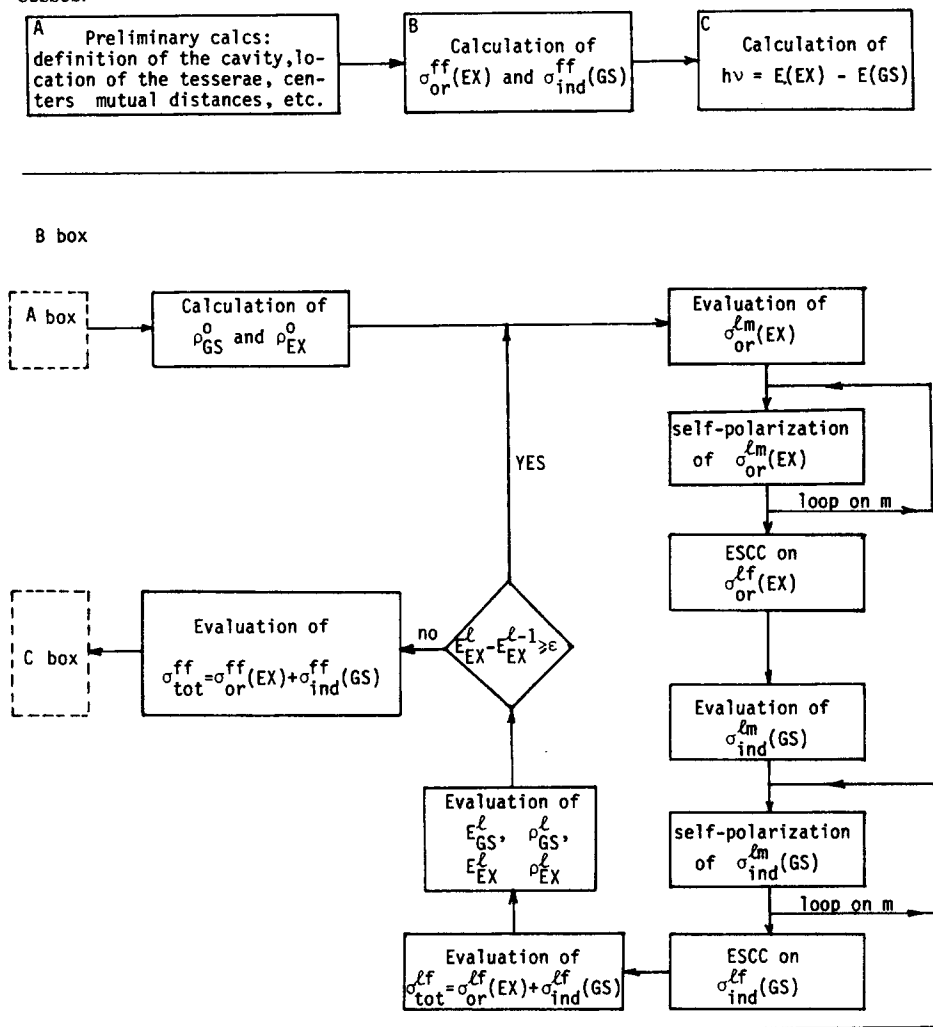
equilibrium with the solvent, to the ground state. These conditions are fulfilled by the phosphorescence spectra and by most cases of fluorescence spectra. Before the emission one has

$$\sigma(\text{EX}) = \sigma_{\text{tot}}(\epsilon, \rho_{\text{EX}}) \qquad (24)$$

and after the emission:

$$\sigma(\text{GS}) = \sigma_{\text{or}}(\rho_{\text{EX}}) + \sigma_{\text{ind}}(n^2, \rho_{\text{GS}}) \qquad (25)$$

The calculations are given at a fixed internal geometry of M, which could be different from that of equilibrium for the GS.

The following computational scheme has been adopted.

4.1. Evaluation of $\sigma_{\text{or}}(\text{EX})$ and $\sigma_{\text{ind}}(\text{GS})$. It is convenient to proceed in parallel in the iterative determination of $\sigma_{\text{or}}^{lf}(\text{EX})$ and $\sigma_{\text{ind}}^{lf}(\text{GS})$ using the couple of wave functions $\psi_{\text{GS}}^{(l)}$ and $\psi_{\text{EX}}^{(l)}$ associated with the approximate Hamiltonian:

$$\hat{H}_M = H_M^0 + V(\sigma_{\text{or}}^{l-1}(\text{EX})) + V(\sigma_{\text{ind}}^{l-1}(\text{GS})) \qquad (26)$$

The first step refers to the *in vacuo* Hamiltonian,

$\hat{H}_M = \hat{H}_M^0$. It may be remarked that equivalent results are obtained, with the same number of cycles, if the first step is related to $\hat{H}_M = \hat{H}_M^0 + V(\sigma_{\text{tot}}(\text{GS}))$.

4.1.1. Evaluation of $\sigma_{\text{or}}^{0f}(\text{EX})$. The procedure and the formulas of 3.1.1 and 3.1.2 are employed, replacing $\rho_M^0(\text{GS})$ with $\rho_M^0(\text{EX})$. After ESCC (3.1.3) the orientational component $\sigma_{\text{or}}^{0f}(\text{EX})$ is obtained (3.1.5). The iterative refinement of $\sigma_{\text{or}}^{0f}(\text{EX})$ (as in 3.1.4) is not performed.

4.1.2. Evaluation of $\sigma_{\text{ind}}^{0f}(\text{GS})$. A formula similar to eq. (22) of 3.2.2 is employed. In the present case the constant term corresponds to

$$\frac{n^2 - 1}{4\pi n^2} \frac{\partial}{\partial n} [V(\rho_{\text{GS}}^0) + V(\sigma_{\text{or}}^{0f}(\text{EX}))] \qquad (27)$$

while the iterative calculation regards the contributions to σ deriving from $\sigma_{\text{ind}}^0(\text{GS})$. At the end of the cycle ($m_{\text{max}} < 4$), ESCC is applied.

4.1.3. Calculations of improved expressions for ψ_{GS} and ψ_{EX}. These wave functions are related to

a Hamiltonian containing the approximations to σ_{or}(EX) and σ_{ind}(GS) obtained in the two preceding steps.

4.2. Final calculations. See the remarks in 3.3.

A diagrammatic description of the computational procedure is given in Table II.

V. TEST CALCULATIONS

The numerical examples presented in this section are addressed only to corroborate the internal consistency of the computational procedure, without any ambition of giving realistic predictions on actual physical systems. To this end, a simple molecular system has been chosen, H_2CO, in two solvents the first characterized by $\epsilon = 80$ and $n^2 = 1.777$, the second by $\epsilon = 2.284$ and $n^2 = 2.244$. All calculations refer to the standard geometry of H_2CO ($R_{CO} = 1.22$ Å, $R_{CH} = 1.08$ Å, $\angle HCH = 120°$) and to the STO-3G basis. In all cases the cavity in the dielectric is composed of four spheres, centered on the nuclei, with radii $R_0 = 1.4$ Å, $R_C = 1.6$ Å, $R_H = 1.2$ Å. The position of the centers of the tesserae corresponds to angular increments $\Delta\theta = \Delta\varphi = 22.5°$. The polar axes for all the spheres are parallel to the molecular axis. A check is introduced in the program that replaces partly overlapping tesserae on adjacent spheres with appropriate connection surfaces.

Table III reports the results of the calculations concerning the absorption process $^1(n \to \pi^*)$. The first set of partial results (cases 1–6) regards the process of self-consistence for the definition of σ_{tot}(GS). The basic test is given in this case by the value of ΔE, defined as the difference in the energies related to the Hamiltonians $\hat{H}_M^0 + \hat{V}(\sigma_{tot}(GS))$ and $\hat{H}_M^0$. This quantity is not the energy change due to the process of solution of one mol of gaseous M,[15] but rather it measures the interaction energy of the solute with a solvent in the correct polarization state. From the trend of the ΔE values, it turns out that stable values are reached at the third cycle. The values of the GS dipole moment confirm this conclusion. It may be also remarked, in passing, that the μ(GS) values indicate that the polarization of the solute is not negligible. In a preceding article[16] the effect of the solvent on the equilibrium geometry of H_2CO has been also tested; the effect is rather modest and it may be discarded in the present computations. In Table III we also give for these partial calculations the value of the excitation energy; these calculations correspond to the approximation made in

Table III. $^1(n \to \pi^*)$ absorption process in H_2CO. [$h\nu = E(EX) - E(GS)$ (eV); $\Delta E = E(sol) - E(vac)$ (kcal/mol).]

Case n.	Surface charge	Solvent 1			
		$h\nu$	$\Delta E(GS)$	$\mu(GS)$	$\mu(EX)$
1	-	4.106	-	1.52	0.54
2	$\sigma_{tot}^{of}(GS)$	4.390	10.27	1.99	0.11
3	$\sigma_{tot}^{1f}(GS)$	4.428	11.93	2.07	0.02
4	$\sigma_{tot}^{2f}(GS)$	4.435	12.24	2.09	0.01
5	$\sigma_{tot}^{3f}(GS)$	4.437	12.31	2.09	0.01
6	$\sigma_{tot}^{4f}(GS)$	4.437	12.31	2.09	0.01
7	$\sigma_{or}^{4f}(GS) + \sigma_{ind}^{of}(EX)$	4.294	8.41	1.92	0.17
8	$\sigma_{or}^{4f}(GS) + \sigma_{ind}^{1f}(EX)$	4.285	8.08	1.90	0.18
9	$\sigma_{or}^{4f}(GS) + \sigma_{ind}^{2f}(EX)$	4.284	8.05	1.90	0.18
10	$\sigma_{or}^{2f}(GS) + \sigma_{ind}^{of}(EX)$	4.292	8.36	1.92	0.17
11	$\sigma_{or}^{2f}(GS) + \sigma_{ind}^{1f}(EX)$	4.284	8.04	1.90	0.18
12	$\sigma_{or}^{1f}(GS) + \sigma_{ind}^{of}(EX)$	4.287	8.13	1.90	0.18
13	$\sigma_{or}^{1f}(GS) + \sigma_{ind}^{1f}(EX)$	4.278	7.81	1.89	0.19
14	$\sigma_{or}^{of}(GS) + \sigma_{ind}^{of}(EX)$	4.256	6.92	1.84	0.24
15	$\sigma_{or}^{of}(GS) + \sigma_{ind}^{1f}(EX)$	4.248	6.63	1.82	0.25

$h\nu$ = E(EX) - E(GS) (eV)
ΔE = E(sol) - E(vac) (Kcal/mol)

Case n.	Surface charge	Solvent 2			
		$h\nu$	$\Delta E(GS)$	$\mu(GS)$	$\mu(EX)$
16	-	4.106	-	1.52	0.54
17	$\sigma_{tot}^{of}(GS)$	4.245	4.78	1.75	0.32
18	$\sigma_{tot}^{1f}(GS)$	4.254	5.13	1.77	0.31
19	$\sigma_{tot}^{2f}(GS)$	4.255	5.15	1.78	0.30
20	$\sigma_{tot}^{3f}(GS)$	4.255	5.16	1.78	0.30
21	$\sigma_{tot}^{4f}(GS)$	4.255	5.16	1.78	0.30
22	$\sigma_{or}^{4f}(GS) + \sigma_{ind}^{of}(EX)$	4.017	-0.61	1.47	0.56
23	$\sigma_{or}^{4f}(GS) + \sigma_{ind}^{1f}(EX)$	4.004	-1.00	1.45	0.58
24	$\sigma_{or}^{4f}(GS) + \sigma_{ind}^{2f}(EX)$	4.003	-1.04	1.44	0.59
25	$\sigma_{or}^{2f}(GS) + \sigma_{ind}^{of}(EX)$	4.017	-0.61	1.47	0.56
26	$\sigma_{or}^{2f}(GS) + \sigma_{ind}^{1f}(EX)$	4.004	-1.00	1.45	0.58
27	$\sigma_{or}^{1f}(GS) + \sigma_{ind}^{of}(EX)$	4.017	-0.61	1.47	0.56
28	$\sigma_{or}^{1f}(GS) + \sigma_{ind}^{1f}(EX)$	4.004	-1.00	1.45	0.58
29	$\sigma_{or}^{of}(GS) + \sigma_{ind}^{of}(EX)$	4.016	-0.65	1.47	0.56
30	$\sigma_{or}^{of}(GS) + \sigma_{ind}^{1f}(EX)$	4.004	-1.01	1.45	0.58

$h\nu$ = E(EX) - E(GS) (eV)
ΔE = E(sol) - E(vac) (Kcal/mol)

preceding articles[13,15] in which the discrimination between orientational and inductive polarization of the solvent had not been introduced. The values of $h\nu$ indicates that stable values are reached at the third step. It must be also remarked that the final value of μ(EX) is practically zero. The following set of partial results (cases 7–15) regard the calculation of σ_{ind}(EX) performed to different levels

of accuracy in σ_{or}(GS). The basic quantity is now $h\nu$ (and μ_{EX}). In all cases the convergence is achieved at the second step; we have not considered it necessary to report further steps that do not produce changes in the digits reported in Table III. It should be clear that ΔE and μ_{GS} in these cases do not have a direct physical meaning, and that they must be considered as nothing more than additional numerical indexes useful to appreciate the effect of the various approximation steps (the correct values of ΔE and μ_{GS} in the present context are given in line 6). Our final result is given in line 9 and it corresponds to a blue shift of 0.178 eV = 4.10 kcal/mol.

The second portion of the Table III regards the nonpolar solvent. Convergence in the polarization of the ground state (see ΔE of cases 16–21) is faster than in the preceding example, because the polarizing power of the solvent is now lower. With this solvent the self-polarization of the solute could be also neglected (compare $h\nu$ in cases 24 and 29). It may be remarked that the convergence in σ_{ind}(EX) is a little lower than in the preceding solvent (see ΔE of cases 22–24).

Table IV regards the $^1(\pi \rightarrow \pi^*)$ absorption process. When the calculations are performed for different electronic states, it is not necessary to repeat every time the computational steps corresponding to cases 1–6. They are in fact completely equivalent to those denoted as cases 1–6 in Table III. The differences in the intrinsic nature of the $^1(\pi \rightarrow \pi^*)$ and $^1(n \rightarrow \pi^*)$ excitation processes are evident when one compares cases 6–8 of Table IV with the corresponding cases of Table III. The promotion of one electron from the π to the π^* orbital produces less changes in the solute charge distribution than the promotion from n to σ^*; of consequence, the substitution of σ_{ind}(GS) with σ_{ind}(EX) has a lower effect on $h\nu$, and the computational procedure gives stable values at the first cycle. These trends are even more evident in solvent 2 (second portion of Table IV). We recall that $^1(\pi \rightarrow \pi^*)$ transitions are relatively badly described by EHP, as well as by single excitation CI methods, especially for the description of the ensuing charge distribution and molecular electrostatic potential (see Daudel et al.[19]).

Tables V–VII report the results concerning emission processes. In all cases stable values are reached at the second step, but also the results of the first step could be safely employed. In these calculations, again the basic result is given by $h\nu$; the values of ΔE(GS) and μ(GS) have not a direct physical meaning.

Table IV. $^1(\pi \rightarrow \pi^*)$ absorption process in H_2CO. [$h\nu = E(EX) - E(GS)$ (eV); $\Delta E = E(sol) - E(vac)$ (kcal/mol).]

Case n.	Surface charge	Solvent 1			
		hν	ΔE(GS)	μ(GS)	μ(EX)
1	-	15.05	-	1.52	0.88
2	σ_{tot}^{of}(GS)	15.05	10.27	1.99	1.00
3	σ_{tot}^{1f}(GS)	15.06	11.93	2.07	1.02
4	σ_{tot}^{2f}(GS)	15.06	12.24	2.09	1.03
5	σ_{tot}^{3f}(GS)	15.06	12.31	2.09	1.03
6	σ_{tot}^{4f}(GS)	15.06	12.31	2.09	1.03
7	σ_{or}^{4f}(GS) + σ_{ind}^{of}(EX)	15.05	11.35	2.03	1.01
8	σ_{or}^{4f}(GS) + σ_{ind}^{1f}(EX)	15.05	11.35	2.03	1.01
9	σ_{or}^{4f}(GS) + σ_{ind}^{2f}(EX)	15.05	11.34	2.03	1.01
10	σ_{or}^{2f}(GS) + σ_{ind}^{of}(EX)	15.05	11.31	2.03	1.01
11	σ_{or}^{2f}(GS) + σ_{ind}^{1f}(EX)	15.05	11.30	2.03	1.01
12	σ_{or}^{1f}(GS) + σ_{ind}^{of}(EX)	15.05	11.12	2.02	1.01
13	σ_{or}^{1f}(GS) + σ_{ind}^{1f}(EX)	15.05	11.11	2.02	1.01
14	σ_{or}^{of}(GS) + σ_{ind}^{of}(EX)	15.04	10.07	1.96	1.00
15	σ_{or}^{of}(GS) + σ_{ind}^{1f}(EX)	15.04	10.07	1.96	1.00

$h\nu$ = $E(EX) - E(GS)$
ΔE = $E(sol) - E(vac)$

Case n.	Surface charge	Solvent 2			
		hν	ΔE(GS)	μ(GS)	μ(EX)
16	-	15.05	-	1.52	0.88
17	σ_{tot}^{of}(GS)	15.05	4.78	1.75	0.94
18	σ_{tot}^{1f}(GS)	15.05	5.13	1.77	0.94
19	σ_{tot}^{2f}(GS)	15.05	5.15	1.78	0.94
20	σ_{tot}^{3f}(GS)	15.05	5.16	1.78	0.94
21	σ_{tot}^{4f}(GS)	15.05	5.16	1.78	0.94
22	σ_{or}^{4f}(GS) + σ_{ind}^{of}(EX)	15.04	4.26	1.71	0.93
23	σ_{or}^{4f}(GS) + σ_{ind}^{1f}(EX)	15.04	4.25	1.71	0.93
24	σ_{or}^{4f}(GS) + σ_{ind}^{2f}(EX)	15.04	4.25	1.71	0.93
25	σ_{or}^{2f}(GS) + σ_{ind}^{of}(EX)	15.04	4.26	1.71	0.93
26	σ_{or}^{2f}(GS) + σ_{ind}^{1f}(EX)	15.04	4.25	1.71	0.93
27	σ_{or}^{1f}(GS) + σ_{ind}^{of}(EX)	15.04	4.26	1.71	0.93
28	σ_{or}^{1f}(GS) + σ_{ind}^{1f}(EX)	15.04	4.25	1.71	0.93
29	σ_{or}^{of}(GS) + σ_{ind}^{of}(EX)	15.04	4.25	1.71	0.93
30	σ_{or}^{of}(GS) + σ_{ind}^{1f}(EX)	15.04	4.24	1.71	0.93

$h\nu$ = $E(EX) - E(GS)$ (eV)
ΔE = $E(sol) - E(vac)$ (kcal/mol)

The computational procedure of Sec. IV may be arranged to give also the absorption and emission energies in the solution model in which the solvent is characterized by ϵ alone. For solvents with a relatively high influence of the orientational contribution to the dielectric constant, as is the case for solvent 1, it is reasonable to assume that during the spectroscopic processes, M is affected by the reaction field of the starting electronic state. So for

Table V. $^1(\pi^* \to n)$ emission process in H_2CO. [$h\nu = E(EX) - E(GS)$ (eV); $\Delta E = E(sol) - E(vac)$ (kcal/mol.]

Case n.	Surface charge	hν	ΔE(GS)	μ(GS)	μ(EX)
		Solvent 1			
1	-	4.106	-	1.52	0.54
2	$\sigma_{or}^{0f}(EX) + \sigma_{ind}^{0f}(GS)$	4.066	2.15	1.60	0.44
3	$\sigma_{or}^{1f}(EX) + \sigma_{ind}^{1f}(GS)$	4.071	2.42	1.62	0.42
4	$\sigma_{or}^{2f}(EX) + \sigma_{ind}^{2f}(GS)$	4.073	2.47	1.62	0.42
5	$\sigma_{or}^{3f}(EX) + \sigma_{ind}^{3f}(GS)$	4.073	2.48	1.62	0.42
		Solvent 2			
6	-	4.106	-	1.52	0.54
7	$\sigma_{or}^{0f}(EX) + \sigma_{ind}^{0f}(GS)$	4.240	4.68	1.75	0.33
8	$\sigma_{or}^{1f}(EX) + \sigma_{ind}^{1f}(GS)$	4.249	5.01	1.77	0.31
9	$\sigma_{or}^{2f}(EX) + \sigma_{ind}^{2f}(GS)$	4.250	5.04	1.77	0.31
10	$\sigma_{or}^{3f}(EX) + \sigma_{ind}^{3f}(GS)$	4.250	5.05	1.77	0.31

$h\nu = E(EX) - E(GS)$ (eV)
$\Delta E = E(sol) - E(vac)$ (Kcal/mol)

Table VII. $^3(\pi^* \to \pi)$ emission process in H_2CO. [$h\nu = E(EX) - E(GS)$ (eV); $\Delta E = E(sol) - E(vac)$ (kcal/mol).]

Case n.	Surface charge	hν	ΔE(GS)	μ(GS)	μ(EX)
		Solvent 1			
1	-	3.928	-	1.52	0.88
2	$\sigma_{or}^{0f}(EX) + \sigma_{ind}^{0f}(GS)$	4.022	9.64	1.93	0.99
3	$\sigma_{or}^{1f}(EX) + \sigma_{ind}^{1f}(GS)$	4.037	10.35	1.97	1.00
4	$\sigma_{or}^{2f}(EX) + \sigma_{ind}^{2f}(GS)$	4.039	10.42	1.97	1.00
5	$\sigma_{or}^{3f}(EX) + \sigma_{ind}^{3f}(GS)$	4.039	10.42	1.97	1.00
		Solvent 2			
6	-	3.928	-	1.52	0.88
7	$\sigma_{or}^{0f}(EX) + \sigma_{ind}^{0f}(GS)$	3.984	4.78	1.75	0.94
8	$\sigma_{or}^{1f}(EX) + \sigma_{ind}^{1f}(GS)$	3.992	5.11	1.77	0.94
9	$\sigma_{or}^{2f}(EX) + \sigma_{ind}^{2f}(GS)$	3.993	5.15	1.77	0.94
10	$\sigma_{or}^{3f}(EX) + \sigma_{ind}^{3f}(GS)$	3.993	5.15	1.77	0.94

$h\nu = E(EX) - E(GS)$ (eV)
$\Delta E = E(sol) - E(vac)$ (Kcal/mol)

the absorption process, the interaction term in the Hamiltonian will be given by $\sigma_{tot}(\epsilon,\rho_{GS})$ and in emission processes by $\sigma_{tot}(\epsilon,\rho_{EX})$. Results analogous to those reported as cases 6 and 21 in Tables III and IV are the absorption energies in this approximation. The emission energy can be obtained by applying the procedure outlined in steps 3.1.1–3.1.4. For solvents for which the dielectric constant is essentially due to electronic polarization contributions, it is reasonable to assume the opposite position, i.e. that in the spectroscopic

processes M feels the reaction field of the final state. Of consequence for the absorption process, the interaction operator will be given by $\sigma_{tot}(\epsilon,\rho_{EX})$ and in the emission process by $\sigma_{tot}(\epsilon,\rho_{GS})$.

The results for the two solvents, given as shifts with respect to the calculation *in vacuo* are reported in Table VIII and compared with the analogous shifts deduced by the results of Tables III–VII. It must be stressed that these results are only indicative, the quality of the computations being rather modest. Apart from these considerations, we point out that a more refined assessment of some features of the model could modify the results to some extent. For example, according to *ab initio* computations on hydration clusters, the cavity in the $>C=O$ region of the $(n \to \pi^*)$ excited states should be enlarged. By repeating the calculation of emission shifts for $^1(\pi^* \to n)$ and $^3(\pi^* \to n)$ states, in solvent 1 with a cavity radius R_0 increased by 0.3 Å, the results are -0.09 kcal/mol and 0.07 kcal/mol (model using ϵ and n^2), and

Table VI. $^3(\pi^* \to n)$ emission process in H_2CO. [$h\nu = E(EX) - E(GS)$ (eV) $\Delta E = E(sol) - E(vac)$ (kcal/mol).]

Case n.	Surface charge	hν	ΔE(GS)	μ(GS)	μ(EX)
		Solvent 1			
1	-	2.971	-	1.52	0.62
2	$\sigma_{or}^{0f}(EX) + \sigma_{ind}^{0f}(GS)$	2.927	2.00	1.59	0.53
3	$\sigma_{or}^{1f}(EX) + \sigma_{ind}^{1f}(GS)$	2.934	2.22	1.61	0.52
4	$\sigma_{or}^{2f}(EX) + \sigma_{ind}^{2f}(GS)$	2.936	2.27	1.61	0.51
5	$\sigma_{or}^{3f}(EX) + \sigma_{ind}^{3f}(GS)$	2.936	2.27	1.61	0.51
		Solvent 2			
6	-	2.971	-	1.52	0.62
7	$\sigma_{or}^{0f}(EX) + \sigma_{ind}^{0f}(GS)$	3.137	4.68	1.75	0.41
8	$\sigma_{or}^{1f}(EX) + \sigma_{ind}^{1f}(GS)$	3.149	5.01	1.77	0.39
9	$\sigma_{or}^{2f}(EX) + \sigma_{ind}^{2f}(GS)$	3.150	5.04	1.77	0.39
10	$\sigma_{or}^{3f}(EX) + \sigma_{ind}^{3f}(GS)$	3.150	5.04	1.77	0.39

$h\nu = E(EX) - E(GS)$ (eV)
$\Delta E = E(sol) - E(vac)$ (Kcal/mol)

Table VIII. Comparison of solvent shifts[a] calculated with and without the distinction between orientational and inductive solvent effects.

		$^1(n \to \pi^*)$	$^1(\pi \to \pi^*)$	$^1(\pi^* \to n)$	$^3(\pi^* \to \pi)$	$^3(\pi^* \to n)$
Solvent 1	ϵ,n^2	4.10	0	-0.76	2.56	-0.81
	ϵ	7.63	0	-5.14	1.78	-6.27
Solvent 2	ϵ,n^2	-2.38	-0.23	3.32	1.50	4.13
	ϵ	-2.47	0	3.44	1.50	4.27

[a] Values in kcal/mol given as difference of the energy transition in the solvent and *in vacuo*.

−3.18 kcal/mol and −3.80 kcal/mol (model using ϵ alone).

It may be of some interest to inspect the computation times. For the H_2CO molecule, the CPU time on a IBM 370/168 computer necessary to get the $^1(n \rightarrow \pi^*)$ absorption energy in a first solvent is $\simeq 64$ sec, and an additional time of 45 sec is necessary to get the absorption energy in a second solvent. The CPU time necessary to get the emission energy is of the same order of magnitude. With the same program (a modified version of GAUSSIAN 70) the in vacuo calculation requires 12 sec. Passing to a solute of larger size, the in solution/in vacuo ratio of CPU times will decrease. In fact, the time consuming steps of the calculations in solutions are (a) the calculation of the inverse of the distances between surface point charges (box A of Table I), which increases approximately as $n^{1.5}$ (n = number of electrons), and (b) the calculation of one-electron integrals corresponding to $\hat{V}(\sigma)$, which increases approximately as $m^2 n^{0.75}$ (m is the dimension of the basis set), while the computation of two-electron integrals, needed in vacuo as well as in solution calculations, increases as m^4.

VI. CONCLUDING REMARKS

The computational scheme considered in this article has been elaborated with the basic aim of supplying a computational tool analogous to those already available for in vacuo ab initio calculations of light absorption and emission processes, but including solvent effects in the framework of the continuum approximation. To this end, attention has been paid to preserve the usual scheme of ab initio programs, introducing in the solute Hamiltonian a realistic and clearly defined interaction operator. The description of the solvent interaction is general enough, and it can be defined to the desired level of accuracy. In fact, the shape of the cavity can be modelled with the desired accuracy, and the precision of the description is directly related to the density of surface charges one selects. These features are supplemented with the separate consideration of the effects due to the orientational and inductive components of the solvent polarization. We are confident that this description of the solvent interaction is realistic enough to justify calculations performed to a relatively high level of accuracy [multiconfiguration (MC) SCF or CI calculations performed over appropriate basis sets].

We have given in the preceding section some numerical results corresponding to a rather crude and approximate application. The relatively poor description of GS and EX states obtained by combining a minimal basis set with simple SCF-like descriptions of the wave functions considerably reduces the quality of the results which, for this reason, cannot be regarded as the final answer given by this method on the solvent shifts in formaldehyde. These results are, however, sufficient, we think, to bring out the technical characteristics of the method and its convergence properties. The analysis of other technical characteristics, such as the dependence of the results on the density of point charges and on the shape and volume of the cavity, has not been reported here, the conclusions being similar to those given in article I for the ground state.

A supplementary remark concerns the use of solvent 1 in the calculations reported above. The macroscopic characteristics of this solvent correspond to those of water, and it is well known that the spectrum of formaldehyde in water is due to a mixture of polymeric material with reaction products of H_2CO with H_2O.[20] Formaldehyde must be considered in this case as nothing more than a model of carbonylic compounds. Carbonylic compounds, on their part, make relatively stable hydrogen-bonded complexes with water. We have remarked in a preceding section that the present computational scheme can be directly applied to a supermolecule $M S_n$, where n molecules of solvent are linked to M through H-bonds. We point out here, however, that there is good evidence that in the GS as well as in the excited states the energetics of H-bonded complexes is sufficiently well reproduced by the electrostatic components of the interaction energy alone.[13,21,22] The different emphasis given to specific hydrogen-bond effects and the orientation of polar solvent molecules in early interpretations of the blue shift of $^1(n \rightarrow \pi^*)$ transitions (compare, e.g., Brealey and Kasha[23] with McConnell[24]) might be less drastic than they appear at first sight. Anyway, the validity of reduction of H-bond interaction to their electrostatic counterpart in solution has not been clearly demonstrated and deserves better scrutiny.

References

1. Y. Ooshika, *J. Phys. Soc. Jpn.*, **9**, 594 (1954).
2. H. C. Longuet-Higgins and J. A. Pople, *J. Chem. Phys.*, **27**, 192 (1957).

3. E. G. McRae, *J. Phys. Chem.*, **61**, 562 (1957).

4. E. Lippert, *Z. Electrochem.*, **61**, 952 (1957).

5. A. Julg, *J. Chim. Phys. Phys. Chim. Biol.*, **54**, 493 (1957).

6. N. G. Bakshiev, *Opt. Spectrosc. USSR*, **10**, 379 (1961).

7. L. Bilot and A. Kawski, *Z. Naturforsch.*, **17A**, 621 (1962).

8. T. Abe. *Bull. Chem. Soc. Jpn*, **38**, 1314 (1965).

9. For detailed reviews see (a) S. Basu, *Adv. Quantum Chem.*, **1**, 145 (1964); (b) W. Liptay, in *Modern Quantum Chemistry*, O. Sinanoglu, Ed., Academic, New York, 1965, Vol. II, p. 173; (c) N. Mataga and T. Kubota, *Molecular Interactions and Electronic Spectra*, Dekker, New York, 1970; (d) A. T. Amos and B. L. Burrows, *Adv. Quantum Chem.*, **7**, 289 (1973).

10. L. Onsager, *J. Am. Chem. Soc.*, **58**, 1486 (1936).

11. S. Miertuš, E. Scrocco and J. Tomasi, *Chem. Phys.*, **55**, 117 (1981).

12. S. Miertuš and J. Tomasi, *Chem. Phys.*, **65**, 239 (1982).

13. R. Cimiraglia, S. Miertuš and J. Tomasi, *Chem. Phys. Lett.*, **80**, 286 (1981).

14. A. J. Duben and S. Miertuš, *Chem. Phys. Lett.*, **88**, 395 (1982).

15. R. Bonaccorsi, C. Ghio and J. Tomasi, *Current Aspects of Quantum Chemistry 1981*, R. Carbò, Ed., Elsevier, Amsterdam, 1982, p. 407.

16. R. Bonaccorsi, R. Cimiraglia, S. Miertuš, and J. Tomasi, *J. Mol. Struct., Theochem.*, **94**, 11 (1983).

17. J. E. Sanhueza, O. Tapia, W. J. Laidlaw, and M. Trsic, *J. Chem. Phys.*, **70**, 3096 (1979).

18. K. Morokuma and S. Iwata, *Chem. Phys. Lett.*, **16**, 192 (1972).

19. R. Daudel, H. Le Rouzo, R. Cimiraglia, and J. Tomasi, *Int. J. Quantum Chem.*, **13**, 537 (1978).

20. T. Bercovici, J. King and R. S. Becker, *J. Chem. Phys.*, **56**, 3956 (1972).

21. S. Iwata and K. Morokuma, *J. Am. Chem. Soc.*, **95**, 7563 (1973).

22. J. Tomasi, *Molecular Interactions*, H. Ratajczak and W. J. Orville-Thomas, Eds., Wiley, 1982, Vol. III, p. 119.

23. G. I. Brealey and M. Kasha, *J. Am. Chem. Soc.*, **77**, 4462 (1955).

24. H. McConnell, *J. Chem. Phys.*, **20**, 700 (1952).